Supporting Information

Resolving segmental polymer dynamics in nanocomposites by incoherent neutron spin-echo spectroscopy

Dafne Musino[1], Julian Oberdisse[1], Bela Farago[2], Angel Alegria[3], Anne-Caroline Genix[1]*

[1] *Laboratoire Charles Coulomb (L2C), Université de Montpellier, CNRS, F-34095 Montpellier, France*

[2] *Institut Max von Laue-Paul Langevin (ILL), 71 Avenue des Martyrs, CS 20156, F-38042 Grenoble Cedex 9, France*

[3] *Departamento de Fisica de Materiales (UPV/EHU) and Materials Physics Center (CSIC-UPV/EHU), Paseo Manuel Lardizábal 5, San Sebastian 20018, Spain*

* *Corresponding author: anne-caroline.genix@umontpellier.fr*

1. BDS data treatment

Data analysis was performed in the so-called additive approach, simultaneously fitting the measured real and imaginary parts of the complex permittivity to the sum of a conductivity term and two Havriliak-Negami (HN) functions for the colloidal and industrial PNC systems. The first HN-function corresponds to is associated with the α-process whereas the second one describes the MWS polarization process at lower frequency. It follows that only one HN function was used for the neat SB. The HN relaxation function is expressed as

$$\Phi^*_{HN} = \frac{1}{[1+(i\omega\tau_{HN})^{\gamma}]^{\delta}} \quad \text{(S1)}$$

where τ_{HN} is the HN characteristic time and γ and δ are shape parameters ranging between 0 and 1. In the HN function describing the α-relaxation, γ and δ were systematically coupled

$$\delta(\gamma) = 1 - 0.812\,(1-\gamma)^{0.387} \quad \text{(S2)}$$

allowing an equivalence between the HN and the Kohlrausch-Williams-Watts (KWW) relaxation function in the frequency range corresponding to the α-loss peak, as evidenced by Alvarez et al. [1-3] The following equations relate the HN parameters to those of the KWW equation

$$\beta^{1.23} = \gamma\,\delta(\gamma) \quad \text{(S3)}$$

$$\log(\tau_W) = \log(\tau_{HN}) - 2.6\,(1-\beta)^{0.5}\exp[-3\beta] \quad \text{(S4)}$$

The BDS data of neat SB, industrial PNC and colloidal PNC together with their fits constrained by eqs S1 and S2 are shown in Figures S1, S2 and S3, respectively.

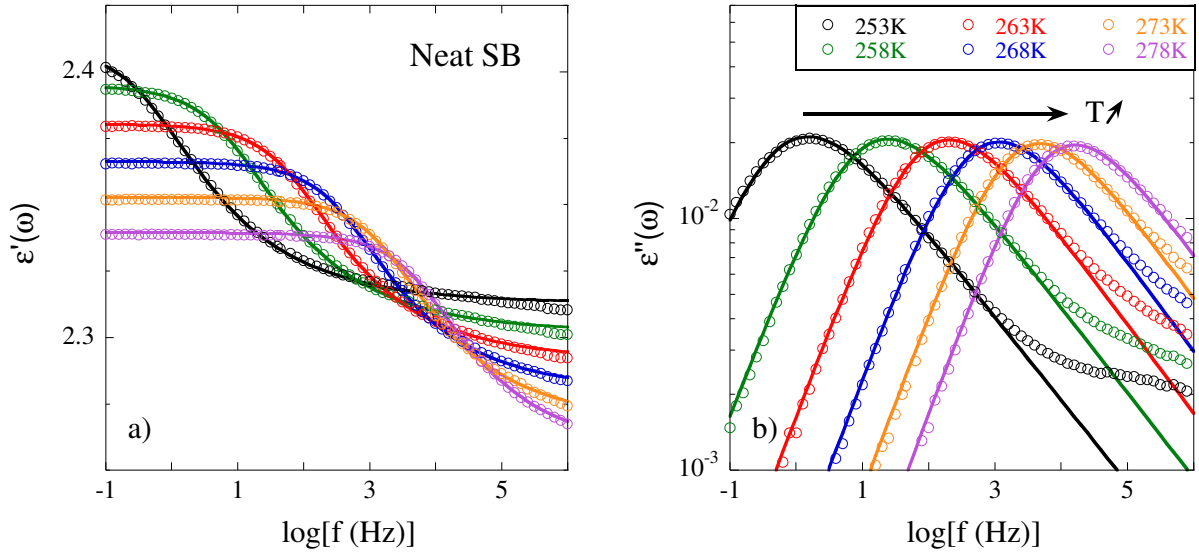

Figure S1. Real **(a)** and imaginary **(b)** parts of the dielectric permittivity measured on neat SB at several temperatures from 253 to 278 K with 5 K-steps. Lines are fits to the experimental data by one Havriliak-Negami function with coupled shape parameters.

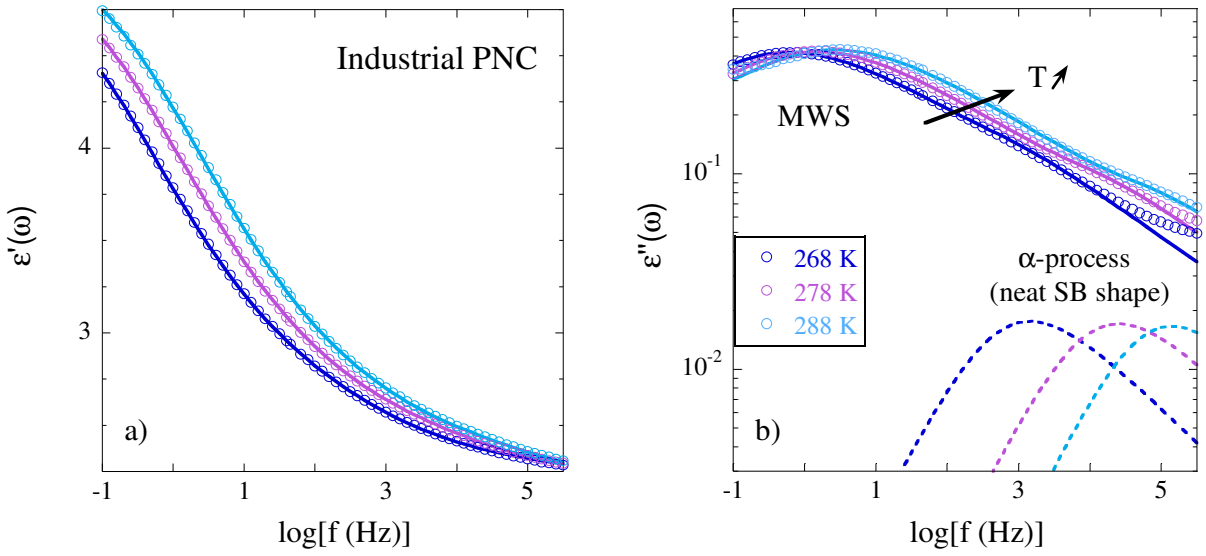

Figure S2. Real **(a)** and imaginary **(b)** parts of the dielectric permittivity measured on industrial SB PNC (Φ_{NP} = 18.3%v) at several temperatures: 268, 278 and 288 K. Lines are fits to the experimental data by two HN functions and conductivity. The shape parameters and the dielectric strength for the α-process are imposed from the neat SB data (modulo a correction for the silica content regarding Δε). The corresponding HN function is shown in b) (dotted lines).

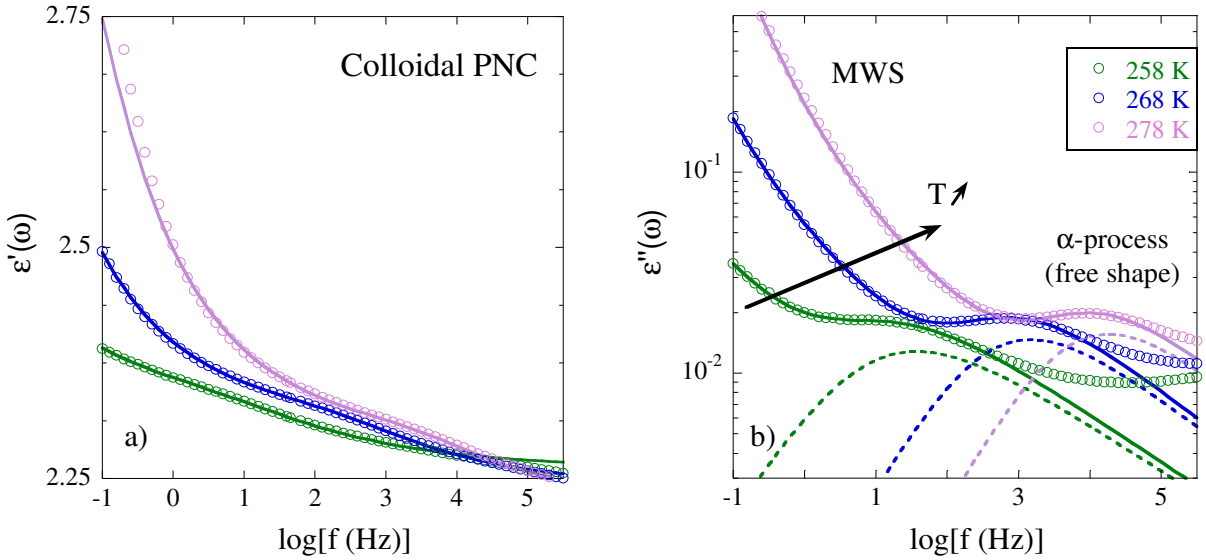

Figure S3. Real **(a)** and imaginary **(b)** parts of the dielectric permittivity measured on colloidal SB PNC (Φ_{NP} = 20.4%v) at several temperatures: 258, 268 and 278 K. Lines are fits to the experimental data by two HN functions and conductivity. The shape parameters are coupled and the dielectric strength is imposed from the neat SB data (modulo a correction for the silica content regarding $\Delta\varepsilon$) for the α-process. The corresponding HN function is shown in b) (dotted lines).

Fit of the α-process by imposing the matrix shape in the colloidal PNC does not lead to a satisfying description of the data as can be seen in Figure S4.

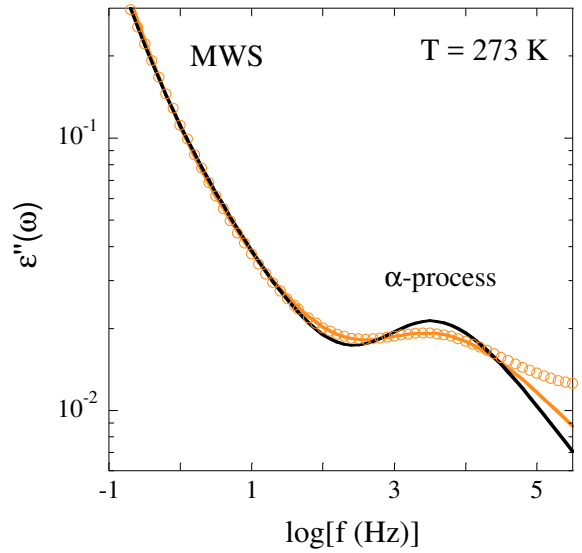

Figure S4. Dielectric loss spectrum at 273 K of the colloidal SB PNC (Φ_{NP} = 20.4%v). Lines are fits to the experimental data by two HN functions and conductivity. The dielectric strength associated with the α-process is imposed from the neat SB data modulo a correction for the silica content and γ is either fixed to the matrix value (γ = 0.72 corresponding to β = 0.44) (black line) or optimized during fitting leading to γ = 0.62 corresponding to β = 0.35 (orange line) – the latter way was used in Figure S3.

2. SANS data

Small-angle neutron scattering (SANS) has been used to confirm the predominance of incoherent scattering in the industrial PNC sample in the q-range above 0.2 $Å^{-1}$. Data are shown in Figure S5.

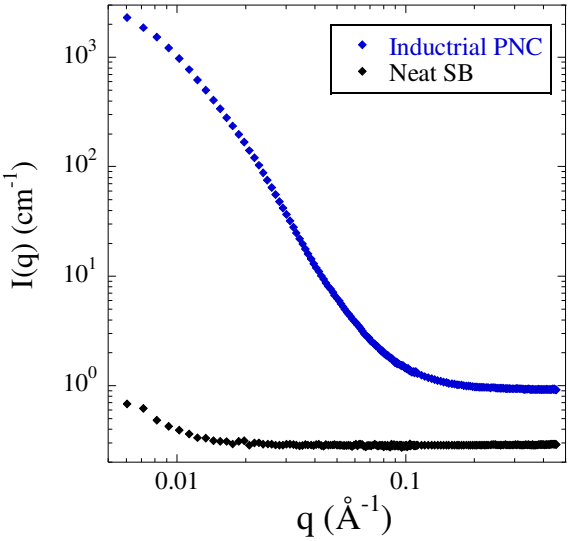

Figure S5. Scattered intensity versus the momentum transfer q for the industrial PNC with 18.3%v of silica and neat SB (data from D22, ILL - France).

3. Complementary NSE results

The KWW times τ_w have been determined from the self-correlation functions in Figure 5 of the article for the neat SB and the industrial PNC using a single β value of 0.55. Their evolution versus q is shown in Figure S6.

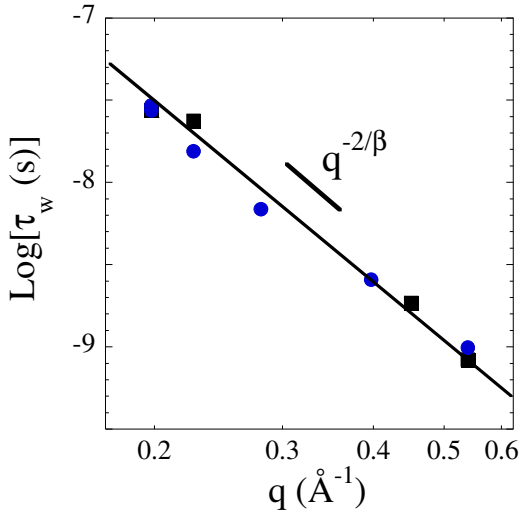

Figure S6. q-dependence of the KWW time scale τ_w at T = 373 K for the matrix (black squares) and industrial PNC (Φ_{NP} = 18.3%v, blue circles).

The NSE data obtained at T = 130°C and q = 0.54 Å^{-1} on an industrial PNC sample with low silica content (Φ_{NP} = 8.3%v) are given in Figure S7 where they are compared to the neat SB and the higher silica concentration PNC. The corresponding decay displays an intermediate time scale confirming the weak but systematic slowing down of the segmental dynamics in industrial PNC samples.

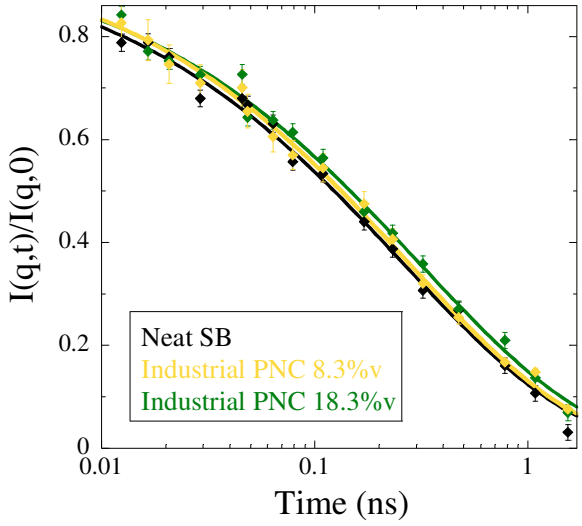

Figure S7. NSE data at T = 130°C and q = 0.54 Å^{-1} for the matrix (black) and industrial PNCs with 8.3%v (yellow) and 18.3%v (green) of silica. Lines are fits using a KWW function decaying to 0 and β = 0.55.

Another confirmation is shown in Figure S8, where one can clearly see that the NSE data measured on the industrial PNC cannot be described by the matrix time scale as it would be if the segmental dynamics were unchanged.

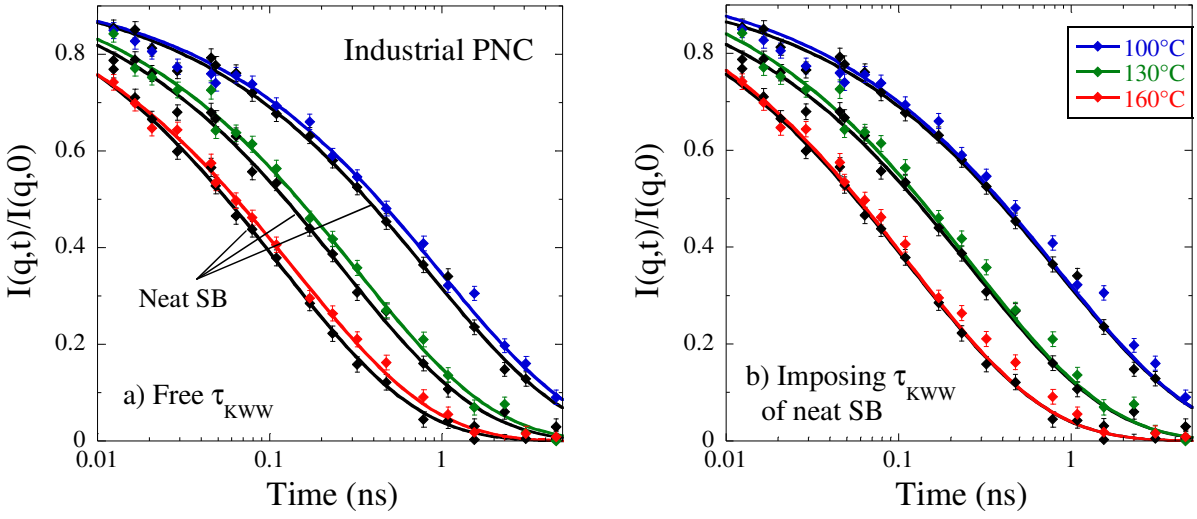

Figure S8. Zoom of the NSE data from Figure 6 at q = 0.54 Å^{-1} for the matrix (black) and the industrial PNC measured at different temperatures. Lines are fits using eq 2 with B(q) = 0 and β = 0.55. The time scale τ_w is either optimized **(a)**, or fixed to the time scale of neat SB **(b)**.

References

(1) Alvarez, F.; Alegra, A.; Colmenero, J., Relationship between the Time-Domain Kohlrausch-Williams-Watts and Frequency-Domain Havriliak-Negami Relaxation Functions. *Phys. Rev. B* **1991,** *44* (14), 7306-7312.

(2) Alvarez, F.; Alegría, A.; Colmenero, J., Interconnection between Frequency-Domain Havriliak-Negami and Time-Domain Kohlrausch-Williams-Watts Relaxation Functions. *Phys. Rev. B* **1993,** *47* (1), 125-130.

(3) Alegría, A.; Colmenero, J.; Mari, P. O.; Campbell, I. A., Dielectric Investigation of the Temperature Dependence of the Nonexponentiality of the Dynamics of Polymer Melts. *Phys. Rev. E* **1999,** *59* (6), 6888-6895.